Concept for polychromatic laser guide stars: one-photon excitation of the $4P_{3/2}$ level of a sodium atom

Jean-Paul Pique, Ioana Cristina Moldovan, and Vincent Fesquet

Laboratoire de Spectrométrie Physique, Université Joseph Fourier, UMR 5588 CNRS-Grenoble I, B.P. 87, 38402 saint Martin d'Hères, France

Received January 3, 2006; accepted May 10, 2006; posted June 26, 2006 (Doc. ID 66841)

One challenge for polychromatic laser guide stars is to create a sufficiently intense source in the UV. The flux required for the measurement of differential tip–tilt is the main issue that we address. We describe a model that has been validated using on-sky data. We present a method that excites the $4P_{3/2}$ sodium level using a one-photon excitation at 330 nm. It is more efficient than the two-photon excitation previously suggested since its power slope flux is 3×10^4 photons/s/m^2/W instead of 1.3×10^3 photons/s/m^2/W. This method is very promising both in terms of flux and system simplicity.

OCIS codes: 010.1080, 010.1330, 020.4180, 030.4070, 140.3610, 260.2510.

1. INTRODUCTION

Near-diffraction-limited imagery on very large telescopes has become a major tool in astrophysics. Adaptive optics (AO) enables these observations if a reference source sufficiently bright to allow wavefront characterization is available within the object's isoplanatic path. The probability of finding such bright sources is the main limitation of AO, especially in the visible (VIS). To increase sky coverage, large astronomical facilities currently use or will implement a monochromatic laser guide star (LGS).[1–5] Important progress was reported in 2006 on a 10 m class telescope at W. M. Keck Observatory. This result[6] showed that AO works well given a 14th magnitude ($\sim2\times10^4$ photons/s/m^2) natural guide star (in this paper, TTNGS will stand for tip–tilt natural guide star) for tip–tilt correction and a 9.5th magnitude ($\sim1.7\times10^6$ photons/s/m^2) LGS for higher-order corrections. This important result has become a reference. The corresponding experimental data will be used often in this paper. At the Keck[7] Observatory a 50 cm laser projector focuses a 17 W (delivered to the top of the telescope), 589 nm laser beam to the mesosphere. The LGS provides the AO phase reference except for the slope θ, its position being indeterminate.[8] The natural TTNGS is needed to measure θ, and, as a result, a further limitation becomes evident: The probability of finding a natural star bright enough is in the best case $\sim10^{-7}$ in the VIS at the galactic poles.[9] The polychromatic laser guide star (PLGS) resolves this major difficulty by creating a multiple wavelength source that consists of the sodium D_2 component and other UV–VIS–IR components collectively referred to in this paper as tip–tilt laser guide stars (TTLGSs). The tip–tilt θ is measured via the differential tip–tilt $\Delta\theta$ between chromatic components. θ is proportional[10] to its derivative $\Delta\theta$ as a function of λ. The French program Etoile Laser Polychromatique pour I'Optique Adaptative (ELP-OA) is probably the only one in the world able to ensure 100% sky coverage. This is essential for very faint astrophysical objects, the priority of decametric optical telescopes (DOT).

The initial proposal[10] to produce a PLGS consisted of exciting the mesospheric sodium atom $4D_{5/2}$ level via the intermediate level $3P_{3/2}$ with two interdependent lasers at 589 and 569 nm. This excitation with classical lasers raised the first problem of intrinsic atomic saturation of the $3S_{1/2}\rightarrow3P_{3/2}$ and $3P_{3/2}\rightarrow4D_{5/2}$ sodium transitions. We overcame the first limitation by developing a modeless laser[11,12] that spreads out the peak power over all velocity classes of the sodium atom. Therefore we hope to gain at least a factor of 10 in the returned flux.[12] In spite of this gain, there is a risk that the returned flux is not sufficient for the ELP-OA program. Indeed, a second limitation comes from the fact that the measurement of $\Delta\theta$ via the TTLGS chromatic components has to be many times more precise than the direct measurement of θ via the TTNGS. The proportionality factor[13] that links θ to $\Delta\theta$ is ~18. The TTNGSs and TTLGSs are both observed in the full field of view of the telescope, and thus their respective performances can be compared. As a result, the photon flux of the TTLGS chromatic components should be 18×18 times (i.e., of ~6 magnitude) more intense than the TTNGS. Keck's and Gemini's engineers[1,14] estimate that the magnitude m_v of a TTNGS cannot exceed an 18th magnitude ($\sim7\times10^2$ photons/s/m^2) and that the magnitude allowing acceptable AO operation is ~16 ($\sim4\times10^3$ photons/s/m^2). McLean and Adkins[7] achieved a Strehl ratio of 36% in the K' band using a 14th (2.6×10^4 photons/s/m^2 magnitude TTNGS. Recent[15] progress has shown that it is possible to achieve the same performance using a 16th magnitude star. Thus we can see that the magnitude of ELP-OA's TTLGS chromatic components magnitude should be less than 12 ($\sim2\times10^5$ photons/s/m^2 and brighter than 10 ($\sim1.3\times10^6$ photons/s/m^2 for good correction. Thus the TTLGS chromatic components have to be almost as in-

tense as the LGS, measured at the Keck Observatory. This is a challenge that requires a precise study of the laser–sodium interaction. The initial proposal to produce a PLGS[10] with two-laser excitation at 589 and 569 nm does not allow the equalization of the 330 and 589 nm fluxes. We demonstrate that the corresponding TTLGS chromatic components are 100 times fainter than the LGS D_2 component. Roughly speaking, if the LGS has a returned flux of $\sim 10^6$ photons/s/m^2, then the TTLGS components will be around 10^4 photons/s/m^2, which are considerably lower than needed. If centroiding algorithms are able to provide significant gains in sensitivity (a factor of 10 seems to be possible[16]), it still remains to find a method to increase TTLGS fluxes by at least 1 order of magnitude.

Thanks to the remarkable properties of the modeless laser[12] that we developed for ELP-OA, we report in this paper a solution that provides a theoretical gain of a factor of 10. It consists of producing independent TTLGSs and LGSs, via a one-photon direct excitation of the $3S_{1/2} \rightarrow 4P_{3/2}$ sodium transition at 330 nm with a modeless laser. Only the use of a modeless laser allows consideration of this possibility. From the point of view of instrumentation, this solution has an important advantage since it preserves many current LGS facilities without any modification. Allowing for atmosphere transmission at 330 nm at Keck's site in Hawaii, we show that a 330 nm modeless laser delivering 1 W at the mesosphere ($\sim$2–3 W at the ground) produces a TTLGS returned flux identical to that obtained by a two-photon excitation using two lasers of 2×15 W (at the mesosphere) at 589 and 569 nm. Ten times higher flux can be obtained with an $\sim$10 W modeless laser at 330 nm. More than 400 W at 589 and 569 nm would be necessary to get this gain. Such high power is problematic at astronomical facilities. The new solution that we propose is simpler and less expensive. It allows spatial–temporal and spectral decoupling of the TTLGSs and LGSs and corresponding lasers. This simplification makes the whole LGS system more robust and reliable.

In this paper we compare the photon flux of the radiative cascade generated by one-photon excitation of the $4P_{3/2}$ level at 330 nm of the sodium atom, with the cascade generated by two-photon excitation of the $4D_{5/2}$ level at 589 and 569 nm for different types of lasers from a theoretical point of view.

2. MODEL

The model that we have used is similar to that described in Ref. 12 for the $3S_{1/2} \rightarrow 3P_{3/2}D_2$ transition. We consider the two cases quoted above.

A. One-Photon Excitation: $4P_{3/2}$ Level One-Photon Direct Excitation at 330 nm

The $4P_{3/2}$ level can be directly excited from the ground state $3S_{1/2}$ with a laser centered at $30,272.51$ cm^{-1} ($\sim$330 nm). Figure 1 presents the energy levels involved in the radiative cascade of the process. The rate equations that describe the atomic system are

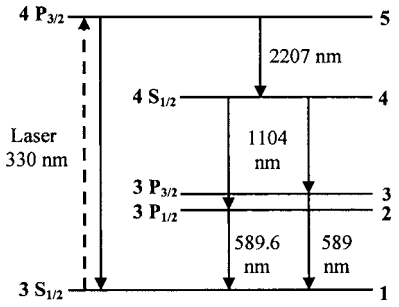

Fig. 1. Energy diagram and relaxation pathways of the one-photon excitation of the $4P_{3/2}$ sodium level at 330 nm.

$$\frac{\partial N_1(t,\mathbf{r},\nu)}{\partial t} = -N_1(t,\mathbf{r},\nu)\frac{g_1}{g_5}\int_{-\infty}^{+\infty}\sigma(\nu'-\nu)\Phi(t,\mathbf{r},\nu')\mathrm{d}\nu'$$

$$+\frac{N_5(t,r,\nu)}{\tau_{51}}+\frac{N_2(t,r,\nu)}{\tau_{21}}+\frac{N_3(t,r,\nu)}{\tau_{31}}$$

$$+N_5(t,r,\nu)\int_{-\infty}^{+\infty}\sigma(\nu'-\nu)\Phi(t,r,\nu')\mathrm{d}\nu', \quad (1)$$

$$\frac{\partial N_2(t,r,\nu)}{\partial t}=\frac{N_4(t,r,\nu)}{\tau_{42}}-\frac{N_2(t,r,\nu)}{\tau_{21}}, \quad (2)$$

$$\frac{\partial N_3(t,r,\nu)}{\partial t}=\frac{N_4(r,t,\nu)}{\tau_{43}}-\frac{N_3(t,r,\nu)}{\tau_{31}}, \quad (3)$$

$$\frac{\partial N_4(t,r,\nu)}{\partial t}=-\frac{N_4(t,r,\nu)}{\tau_{43}}-\frac{N_4(t,r,\nu)}{\tau_{42}}-\frac{N_5(t,r,\nu)}{\tau_{54}}, \quad (4)$$

$$\frac{\partial N_5(t,r,\nu)}{\partial t}=N_1(t,r,\nu)\int_{-\infty}^{+\infty}\sigma(\nu'-\nu)\Phi(t,r,\nu')\mathrm{d}\nu'$$

$$-\frac{N_5(t,r,\nu)}{\tau_{54}}-\frac{N_5(t,r,\nu)}{\tau_{51}}-N_5(t,r,\nu)$$

$$\times\frac{g_1}{g_5}\int_{-\infty}^{+\infty}\sigma(\nu'-\nu)\Phi(t,r,\nu')\mathrm{d}\nu', \quad (5)$$

$$\sum_{i=1}^{5}N_i(t,r,\nu)=N_D(\nu)=N_1(t=0,r,\nu), \quad (6)$$

where

t=time (s),

r=vector of the radial position in the laser beam (m),

ν=frequency Doppler shift (Hz),

g_1, g_5=degeneracies of the $3S_{1/2}$ and $4P_{3/2}$ states, respectively,

$1/\tau_{ij}$=probability of the transition $i \rightarrow j$ (s^{-1}),

Φ=laser photon flux density per unit area, unit time, and unit frequency (m^{-2} s^{-1} Hz^{-1}),

σ=homogeneous absorption cross section (m^2),

N_i=population of the level i,

N_D=Doppler population distribution assuming a uniform temperature at the mesosphere across the laser beam.

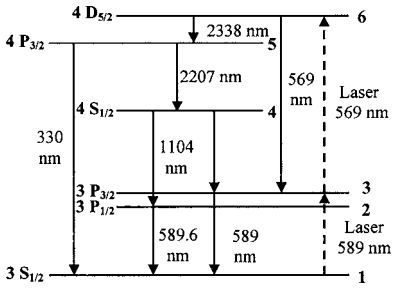

Fig. 2. Energy diagram and relaxation pathways of the two-photon excitation of the $4D_{5/2}$ sodium level at 589 and 569 nm.

The three terms of Eq. (1) correspond to absorption, spontaneous, and stimulated emissions. Using the same hypotheses as in Ref. 12, we define the spatial–temporal saturation parameter to be

$$S(t,r,\nu) = \tau_{51}\int_{-\infty}^{+\infty} \sigma(\nu'-\nu)\Phi(t,r,\nu')\mathrm{d}\nu' = \tau_{51}\varphi(t)D(r)\sigma_{\mathrm{eff}}(\nu). \tag{7}$$

The effective cross section $\sigma_{\mathrm{eff}}(\nu)$ is the convolution product of the homogeneous absorption cross section $\sigma(\nu)$ of the sodium atom and the normalized laser line shape $g(\nu)$. The homogeneous absorption has a Lorentzian profile:

$$\sigma(\nu) = \frac{\sigma_0(\Delta\nu/2)^2}{(\nu_0-\nu)^2+(\Delta\nu/2)^2}, \tag{8}$$

where σ_0 is the homogeneous cross section centered at ν_0, and ν_0 is the frequency line center. $\Delta\nu$ is the homogeneous linewidth of the transition.

$D(r)$ is the laser photon flux distribution per unit area. To reduce the calculation time, a commonly used approximation consists of taking $D(r)$ constant over the diameter $2w$ of the laser beam. In practice, phase mirrors allow this spatial laser beam profile. We approximate the temporal laser pulse width $\varphi(t)$ by a rectangle function of width τ_L. Consequently we have

$$S(t,\nu) = N_L\frac{\tau_{51}}{\tau_L}\frac{\sigma_{\mathrm{eff}}(\nu)}{\pi w^2}, \quad 0<t<\tau_L,$$

$$S(t,\nu) = 0, \quad t<0,\ t>\tau_L, \tag{9}$$

where $N_L=E/h\nu$ is the photon number in a laser pulse and $E=P_\lambda/f_L$ is the pulse energy (where P_λ is the mean laser power at wavelength λ).

The Doppler distribution can be written as

$$N_D(\nu) = N_D^0\frac{2\sqrt{\ln(2)/\pi}}{\Delta\nu_D}\exp\left[-\left(\frac{2\sqrt{\ln(2)}}{\Delta\nu}\nu\right)^2\right], \tag{10}$$

where $N_D^0=\rho\Delta z^{-1}$ is the atomic density by unit volume, ρ is the column density, and Δz is the column height.

B. Two-Photon Excitation of the $4D_{5/2}$ Level at 589 and 569 nm via the $3P_{3/2}$ Level

Figure 2 shows the method of excitation and the radiative cascade induced by two lasers at 589 and 569 nm locked on the transitions $3S_{1/2}\rightarrow 3P_{3/2}$ and $3P_{3/2}\rightarrow 4D_{5/2}$. The formalism used is the same as described above. Two effective cross sections are involved, σ_{01} and σ_{02}, corresponding to *the* $3S_{1/2}\rightarrow 3P_{3/2}$ and *the* $3P_{3/2}\rightarrow 4D_{5/}$ transitions. We will not describe here the rate equation system, which is obvious.

3. RETURNED FLUORESCENCE PHOTON FLUX

A. Calculation of Returned Flux

Neglecting nonradiative processes, the fluorescence flux of the TTLGS chromatic component corresponding to the i toward the j level transition is[12]

$$\Phi_{ij} = Tf_L\frac{A\Delta z}{4\pi z^2}\frac{1}{\tau_{ij}}\int_{-\infty}^{+\infty}\mathrm{d}\nu\int_{-\infty}^{+\infty}\mathrm{d}^2r\int_{\mathrm{pulse}}N_i(r,t,\nu)\mathrm{d}t$$
$$= Tf_L\frac{A\Delta z}{4\pi z^2}\frac{1}{\tau_{ij}}\pi w^2\int_{-\infty}^{+\infty}\mathrm{d}\nu\int_{\mathrm{pulse}}N_i(t,\nu)\mathrm{d}t, \tag{11}$$

where Δz is the thickness and z is the height of the sodium layer, A is the receiver area at the ground (fixed to 1 m^2 in the following), T is the atmospheric transmission at the wavelength corresponding to the transition $i\rightarrow j$, and f_L is the laser repetition rate.

The simulation was carried out for three types of laser line $g(\nu)$:

(1) Laser of type I: a Gaussian line shape of width $\Delta\nu_L=1$ MHz simulating a longitudinal single-mode laser.

(2) Laser of type II: the same line as above, followed by a double phase modulation at 180 and 325 MHz to generate side modes.[12]

(3) Laser of type III: a Gaussian line shape of width $\Delta\nu_L=2.8$ GHz (at $1/e^2$) for $3S_{1/2}\rightarrow 3P_{3/2}$ and $3S_{1/2}\rightarrow 4P_{3/2}$ transitions and $\Delta\nu_L=1$ GHz for transition $3P_{3/2}\rightarrow 4D_{5/2}$; this spectral line shape simulates a modeless laser that excites all velocity classes of the sodium Doppler–hyperfine profile.[12] It is well known that the hyperfine structure of the $3S_{1/2}$ level is 1.77 GHz.

Table 1. Mesospheric Sodium Atom Parameters[a]

Parameter	One-Photon Excitation	Two-Photon Excitation	Unit
τ_{21}	32	32	ns
τ_{31}	16	16	ns
τ_{42}	40	40	ns
τ_{43}	40	40	ns
τ_{51}	320	320	ns
τ_{54}	160	160	ns
τ_{63}	—	75	ns
τ_{65}	—	150	ns
σ_0	4×10^{-14}	—	m^2
σ_{01}	—	1.14×10^{-13}	m^2
σ_{02}	—	1.47×10^{-14}	m^2
Δz	10^4	10^4	m
z	9×10^4	9×10^4	m

[a]See Ref. 10.

The different atomic parameters used in this paper are summed up in Table 1. In spite of a few divergences found in the literature, the transition probabilities $1/\tau_{ij}$ and homogeneous absorption cross sections σ_0 and σ_{0i} have been taken equal to those of Ref. 10.

Sodium density N_D^0 is the most important source of dispersion in experimental results. Indeed, Megie *et al.* showed[17] that seasonal variations of the sodium column density $\rho=\Delta z N_D^0$ is maximum in November and December, about 8×10^9 atoms/cm^2, and minimum in May and June, about 2×10^9 atoms/cm^2, that is to say, a seasonal variation of a factor of 4. Sodium concentration can also depend on the site. Moreover, Kwon *et al.*[18] observed during the winter of 1987 at Mauna Kea Observatory (Hawaii) sporadic sodium enhancement of ~40 min duration that produced sharp sodium abundance peaks of around 6.7×10^9 atoms/cm^2, whereas the mean value was around 3.5×10^9 atoms/cm^2. A detailed study was carried out by Michaille *et al.*[19] at La Palma from September 1999 to August 2000 and showed that the probability of sporadic events is ~1 per night, on time scales varying from a few seconds to a few hours. The authors concluded that the origin of the sporadic events is still uncertain but that the operation of AO systems is affected at least in defocus. The mean value of sodium column density measured by the authors at La Palma is about 4×10^9 atoms/cm^2. Gardner and Shelton[20] also showed that tropospheric gravity waves propagate in the mesosphere creating spatial modulation of the sodium column density capable of changing the local value by 100% in a few hours. In conclusion, all the results found in the literature show that the mean value of the sodium column density is $\rho\approx4\times10^9$ atoms/cm^2 ($N_D^0=4\times10^9$ atoms/m^3 for a column height of $\Delta z=10$ km). As Φ_{ij} is proportional to the column density $\rho=\Delta z N_D^0$, the value of Δz does not have any effect in the calculations that we present in this paper.

The simulation was implemented using MATLAB. Neglecting coherence effects, the following calculations take into account each of the frequencies ν with a step of $\Delta\nu=1$ MHz. The convergence process has been approached carefully. The numerical calculation of the population state has been carried out with an adaptive step integrator. The initial population condition is given for each frequency ν by the distribution $N_D(\nu)$.

B. Required Flux

To estimate the required flux, we have used the results of LGS and TTNGS magnitudes published by researchers at Keck.[6,7] Until now, this is the only complete experimental setup that is working on a 10 m telescope facility. A LGS of magnitude $m_V^{\mathrm{LGS}}=9.5$ been obtained with 10–20 W laser power (typically 17 W) measured at the top of the telescope. Taking into account atmospheric losses, estimate that 15 W is projected into the mesosphere. As we said above, good tip–tilt correction is ensured by a natural TTNGS of magnitude $m_V^{\mathrm{TTNGS}}\approx16$. It is more convenient to work in terms of the number of photons per second and unit area. Consequently, the following conversion[21] is used:

$$m_V=-2.5\log_{10}\frac{\Phi}{\Phi_0}, \tag{12}$$

with Vega as the reference star $\Phi_0=2.54\times10^{-10}$ lumens/cm^2, i.e., in band V centered at 555 nm $\Phi_0=1.043\times10^{10}$ photons/s/m^2.

Thus we calculate for the LGSs and TTNGS's

$$m_V^{\mathrm{LGS}}=9.5\Rightarrow\Phi_{\mathrm{LGS}}=1.7\times10^6\ \text{photons/s/m}^2,$$

$$m_V^{\mathrm{TTNGS}}=16\Rightarrow\Phi_{\mathrm{TTNGS}}=4.2\times10^3\ \text{photons/s/m}^2. \tag{13}$$

Tip–tilt correction requires a TTNGS of a relatively low intensity. But the UV–VIS–IR chromatic components of a TTLGS need much higher intensity. Indeed, the relation between the tip–tilt θ and the differential tip–tilt $\Delta\theta$ is[10,13]

$$\theta=\frac{n_3-1}{n_2-n_1}\Delta\theta\approx18\times\Delta\theta, \tag{14}$$

where n_3 is the average value of the refractive index of air at the observation wavelength and n_2 and n_1 are the indices at the TTLGS chromatic components. The measurement of $\Delta\theta$ has to be 18 times more precise than the measurement θ. Assuming a photon noise limit, the intensity of the TTLGS chromatic components has to be $18^2=324$ times greater than the intensity of the TTNGS. The required photon flux is therefore $\Phi_{\mathrm{TTLGS}}=324\times\Phi_{\mathrm{TTNGS}}\approx1.4\times10^6$ photons/s/m$^2\approx\Phi_{\mathrm{LGS}}$. In other words the intensity of the UV–VIS–IR chromatic component of the TTLGS must be the same order of magnitude as the LGS intensity (D_2 component). We show below that this is impossible using the two-photon excitation.

Other considerations must also be taken into account. For example, the LGS spot is larger on the sky than a natural tip–tilt star spot, roughly by $\sqrt{2}$ in theory due to the laser going both up and down through the atmosphere, and in practice as seen so far at Lick, Keck, Gemini, and the Very Large Telescope at the European Southern Observatory by a factor of 2. This will result in a factor of 4 increase in power requirement to get the same centroiding accuracy as a natural star. A major gain can be achieved by AO correcting both upgoing and return laser beams. This has been pursued in initial experiments at the U.S. Air Force Starfire Optical Range.[22]

We conclude that a TTLGS chromatic component flux of ~10^6 photons/s/m^2 at 330 nm is at least necessary for the ELP-OA project.

C. Validation of the Model Based on Keck, PASS-2, and PASS-1 Experimental and Theoretical Results

To reproduce the photon flux of the LGS obtained at Keck, we have run our simulation program for the two-photon excitation, considering the power of the second laser $P_{569}=0$, $f_L=26$ kHz, and $\tau_L=100$ ns. The mean sodium column density has been taken equal to the value measured at Mauna Kea Observatory[18] ($\rho=4\times10^9$ atoms/cm^2). Taking into account the atmospheric transmission in Hawaii, the laser power P_{589} at the mesosphere at 589 nm was equal to ~15 W. The waist value $w=0.4$ m (see below) has

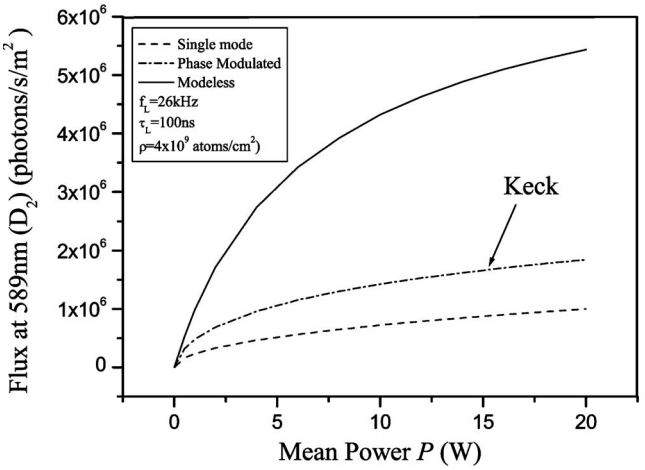

Fig. 3. Returned fluorescence flux at 589 nm (Φ_{31}, LGS) versus average laser power (at the mesosphere) with Keck's laser characteristics for three types of lasers: (i) 1 MHz single longitudinal mode (dashed curve), (ii) 1 MHz single longitudinal mode followed by a double phase modulation at 180 and 325 (dashed–dotted curve), (iii) modeless (solid curve). The arrow corresponds to the typical laser power and returned flux of Keck Observatory. This calculation corresponds to the two-photon excitation. It shows a gain of 6 from single mode to modeless excitation.

been taken to be compatible with the measurements of Keck's LGS shape.[7] Figure 3 displays the results for the three types of lasers presented above. We note the favorable evolution of the intensity of the LGS, when moving from a single-mode laser or a phase-modulated laser to a modeless laser. This behavior has already been experimentally measured and theoretically calculated.[12] Our calculation gives a LGS flux of 1.6×10^6 photons/s/m^2 for the experimental conditions of Keck Observatory. This value has an excellent agreement with the measurement of Keck[7] $m_V\sim9.5$ (1.7×10^6 photons/s/m^2).

In the ELP-OA project, the sky photometry experiment of PASS-2 (Pierrelatte, France)[23–25] provided a comparison of the photon flux at 330 nm versus the laser power at 589 and 569 nm for type I and II lasers. Table 2 and Figs. 4 and 5 compare the experimental results of PASS-2 with our theoretical calculation of the two-photon excitation, with $P_{589}=P_{569}$. The sodium column density during the PASS-2 experiments was not measured. The calculation of the Φ_{51} flux at 330 nm was carried out for a mean sodium column density of $\rho=4\times10^9$ atoms/cm^2. Laser power for the PASS-2 experiments is taken at the ground. Thus for laser beam attenuation, an atmospheric transmission equal to $T=0.8$ has been used. The experimental values considered are the averaged values of the published results, corresponding to a total laser power at the ground $P=P_{589}+P_{569}$ of ~20 and 100 W for the type II laser and 14 W for the type I laser. At the ground, the area of the near-field laser beams is a rectangle of 28 mm $\times$35 mm. To maintain the same near-diffraction area at the mesosphere using the laser shape definition of our calculation, we have considered a waist w of 1 m. A factor of less than 2 is obtained for PASS-2 experiments, between the experiment and our calculation (see Table 2 and Figs. 4 and 5), in good agreement, considering the hypothesis and experimental conditions.

The photometry experiment of PASS-1[26] was realized with Lawrence Livermore National Laboratories (LLNL) lasers [the atomic vapor laser isotope separation (AVLIS) project] in the two-photon excitation. The laser experimental setup is described in Ref. 27. Table 3 summarizes the experimental parameters. Taking into account atmospheric transmission at the LLNL, the average laser power at the mesosphere, $P=P_{589}+P_{569}$, was estimated to be 280 W during the experiment. Variable parameters were the repetition rate (4.3–12.9 kHz), the laser power ratio $P_{569}/(P_{589}+P_{569})$ (30%, 50%, and 70%), and the laser linewidth at 589 nm (1–3 GHz). The set of results has shown a Φ_{51} returned flux at 330 nm that presents little variation between 2.1×10^5 photons/s/m^2 and 5.1×10^5 photons/s/m^2 (Fig. 4 of Ref. 26). We based our calculations for type II and III lasers on sodium column density $\rho=4.1\times10^9$ atoms/cm^2 and laser power ratios 30%, 50%, and 70%. In the PASS-1 experiment the laser beam area at the mesosphere is supposed to be ~1 m^2 with a

Table 2. Parameters of the PASS-2 Experiment and Simulation[a]

Parameter	PASS-2			This Work		
Laser type	I	II	III	I	II	III
f_L (KHz)	5	5	5	5	5	5
τ_L (ns)	35	35	35	35	35	35
w (m)	1	1	1	1	1	1
ρ (atoms/cm^2)	NC[b]	NC	NC	4×10^9	4×10^9	4×10^9
$P=P_{589}+P_{569}$ (W)	~20	~100	~14	$20\times T$	$100\times T$	$14\times T$
Φ_{330} (photons/s/m^2)	4800	26,000	2400	8500	18,300	2900

[a]The laser powers indicated for PASS-2 are ground powers. T is the atmospheric transmission at 589 and 569 nm, which is supposed to be 0.8 at Pierrelatte.

[b]NC, not communicated.

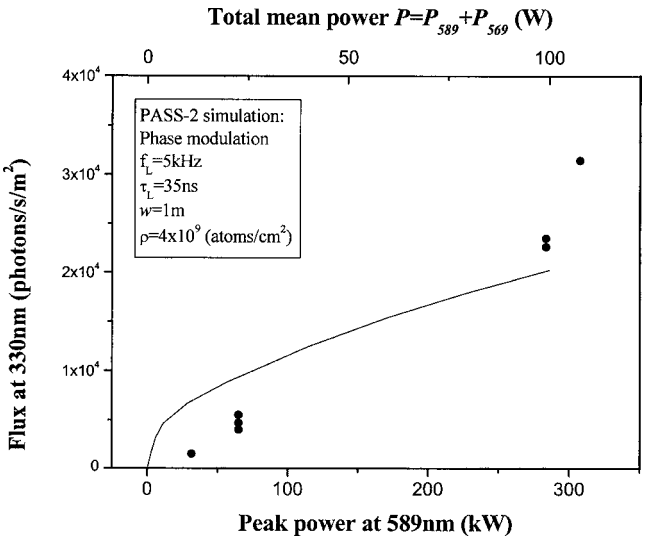

Fig. 4. Returned flux at 330 nm of the PASS-2 experiments at Commissariat à l'Energie Atomique, Pierrelatte (see Ref. 25), versus the peak power at 589 nm ($=P_{589}/f_L\tau_L$) and total mean power ($P_{589}+P_{569}$). The dots correspond to the experimental results using type II lasers and the solid curve corresponds to the numerical simulation in the two-photon excitation with a sodium column density of 4×10^9 atoms/cm^2.

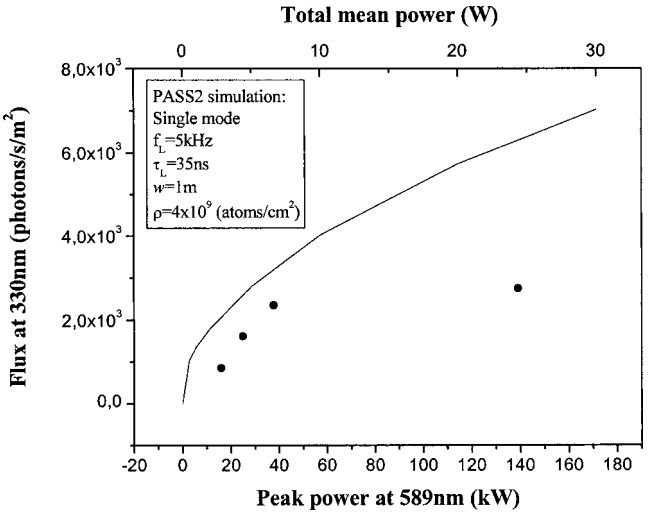

Fig. 5. Experimental and simulated results of PASS-2 with type I lasers.

Table 3. Parameters of the PASS-1 Experiment and Simulation

Parameter	PASS-1[a]	This Work		
Laser type	NC[b]	II	III	III
f_L (kHz)	4.3–12.9	12.9	12.9	12.9
τ_L (ns)	32	32	32	32
$\Delta\nu_L$ (GHz) at 589 nm	1–3	3	3	3
$\Delta\nu_L$ (GHz) at 569 nm	1	1	1	1
ρ (atoms/cm^2)	4.1×10^9	4.1×10^9	4.1×10^9	4.1×10^9
w(m)	0.56	0.56	0.56	1.0
$P=P_{589}+P_{569}$ (W)	280	280	280	280
Φ_{330} (photons/s/m^2)				
$P_{569}/P=30\%$	$2.1–4.2\times10^5$	2.5×10^4	1.2×10^5	2.5×10^5
50%	$2.0–5.1\times10^5$	3.1×10^4	1.3×10^5	3×10^5
70%	$2.8–4.0\times10^5$	3.6×10^4	1.4×10^5	3.2×10^5

[a]Ref. 26.

[b]NC, not communicated.

Fried parameter r_0 of 6 cm (Ref. 26); this corresponds to our model of a beam waist w of 0.56 m. But in Ref. 27, the measured beam area for the same experimental setup was 3.14 m^2, which gives a waist w of 1 m. Knowledge of the beam area is critical because with 280 W of laser power the saturation of the sodium transitions involved is strong, even with a modeless laser. Table 3 shows the calculation with $w=0.56$ m for type II and III lasers and with $w=1$ m for type III lasers. This result clearly shows that the laser used at LLNL was equivalent to a type III laser, i.e., that the laser linewidth covered the sodium Doppler–hyperfine profile continuously, as is mentioned in Ref. 26. The ALVIS lasers remain confidential. We do not know what kind of modulator and applied voltage function were used, but we believe that the LLNL lasers had the same efficiency as our modeless laser,[12] i.e., all sodium velocity classes in the mesosphere were excited according to Ref. 26. The last column of Table 3 shows good agreement between experimental results and our theoretical approach. For waist $w=1$ m and type III lasers of 280 W, total mean power, the returned flux is about 3×10^5 photons/s/m^2.

Our model is also in good agreement with two theoretical works using density-matrix methods. It has been demonstrated[28] that, in the two-photon excitation scheme, taking 2×25 W lasers whose linewidth is assumed to cover all velocity classes of sodium atoms (equivalent to our modeless laser) and taking an atomic column density of 5×10^9 atoms/cm^2, a returned flux of 10^5 photons/s/m^2 (1000 photons per integration time of 10 ms) is obtained. Using the same laser power and sodium density, our model gives a flux of 0.92×10^5 photons/s/m^2, which is very close. Moreover, in the two-photon excitation scheme using a density matrix and Bloch equation approach, it has been clearly shown[29] that the flux at 330 nm is 100 times weaker that the returned flux on the D_2 line (see Fig. 3 of Ref. 29). We discuss this last important result in Subsection 3.D and Fig. 8.

As a result, we conclude on three points: (i) the experimental LGS and PLGS fluxes measured at Keck, PASS-1, and PASS-2 validate our model; (ii) our model agrees well with previous two-photon excitation theoretical models; (iii) two 589 and 569 nm modeless lasers (type III) of total power $P=280$ W (at the mesosphere) will produce a returned flux at 330 nm between 2×10^5 photons/s/m^2 and 5×10^5 photons/s/m^2. This flux is close to that required (see Subsection 3.B), but with laser powers that will be difficult to install at an astronomical telescope.

D. Returned Flux Comparison between the One-Photon and Two-Photon Excitations

In the following, the repetition rate and the laser pulse width were fixed at the current nominal values of the ELP-OA project: $f_L=17$ kHz and $\tau_L=50$ ns. As we noted before, the laser beam spatial shape $D(r)$ is approximated as a rectangular function, with a circular waist w. Several international LGS and PLGS projects recommended a 50 cm diameter projector for a good astronomical site ($r_0\sim10$ cm at 500 nm). Therefore, in this paper the waist value w has been chosen to be compatible with Keck measurement of the full width at half-maximum LGS angular diameter $\alpha=1.4$ arc sec obtained with a 50 cm diameter projector and a near-diffraction laser beam. According to the spatial shape definition considered in our calculation, the waist is $w=[tg(\alpha)z]/[2\sqrt{\ln(2)}]\approx0.4$ m.

Figure 6 displays the photon flux Φ_{51} at 330 nm in the one-photon excitation (curves 4, 5, 6) and two-photon excitation (curves 1, 2, 3). The flux for the other TTLGS wavelengths can be deduced as follows: $\Phi_{51}=(1/2)\Phi_{54}=\Phi_{43}=\Phi_{42}=\Phi_{21}$ in the one-photon or two-photon excitations, and $\Phi_{51}=\Phi_{31}$ in the one-photon excitation. In the two-photon excitation, D_2 transition flux Φ_{31} is essentially due to the one-photon excitation–relaxation process at 589 nm (LGS). In Fig. 6, P corresponds to the total laser power $P_{589}+P_{569}$ with $P_{589}=P_{569}$ in the two-photon excitation, or to the UV laser power P_{330} in the one-photon excitation. Considering that the atmospheric transmission is strongly dependent on the astronomical site, the laser powers used in this subsection are at the mesosphere. The power of 30 W VIS corresponds to the current ELP-OA project; i.e., two 20 W lasers of type III at 589 and 569 nm

Table 4. Simulation of the Returned Flux at 330 nm for Different Laser and Excitation Situations[a]

Parameter	C_1	C_2	C_3	C_4	C_5	C_6	C_7	C_8	C_9
Laser type	I	II	III	I	II	III	III	III	Quasi-cw
f_L(kHz)	17	17	17	17	17	17	17	17	—
τ_L (ns)	50	50	50	50	50	50	50	50	—
$P=P_{589}+P_{569}$ (W)	30	30	30	—	—	—	400	—	—
$P=P_{330}$ (W)	—	—	—	1	1	1	—	10	10
Φ_{330} (photons/s/m^2)	4×10^3	8×10^3	4.2×10^4	3.4×10^3	1.2×10^4	4.2×10^4	1.8×10^5	3×10^5	4.5×10^5
$\gamma(C_i/C_l)$	1	2	11	0.85	3	11	45	75	113

[a] ρ and w are, respectively, fixed to 4×10^9 atoms/cm^2 and 0.4 m.

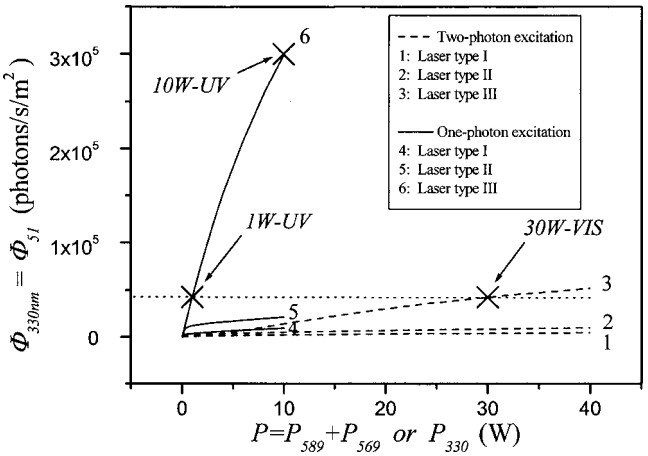

Fig. 6. Return fluorescence flux at 330 nm versus average laser power for the three types of lasers: (a) 1 MHz single-mode laser (curves 1 and 4), (b) 1 MHz single-mode laser followed by a double phase modulation at 180 and 325 MHz (curves 2 and 5), and (c) modeless laser (curves 3 and 6). Solid curves correspond to one-photon excitation at 330 nm and dashed curves to the two-photon excitation at 589 and 569 nm. The cross at 30 W VIS on curve 3 corresponds to the ELP-OA project. The cross at 1 W UV on curve 6 corresponds to UV laser power at 330 nm that matches the flux of photons of the ELP-OA project. The cross at 10 W UV on curve 6 corresponds to the flux that is close to the required flux. For the 10 W in the one-photon excitation, it gives seven times more flux than 30 W in the two-photon excitation.

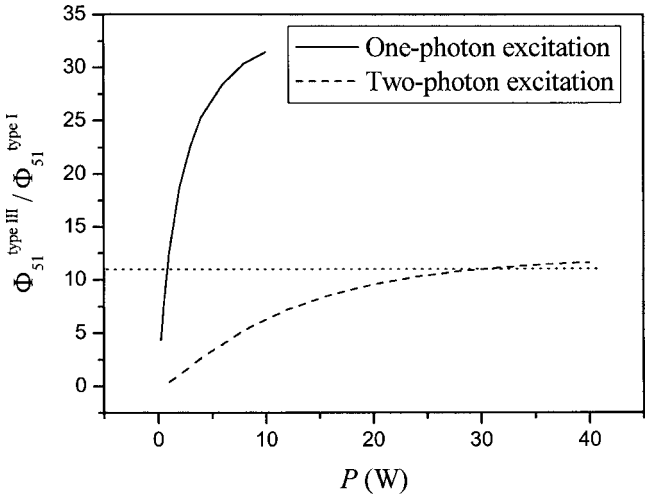

Fig. 7. Ratio between the returned flux at 330 nm for a modeless laser excitation and for a single-mode laser in the one-photon and two-photon excitations as a function of laser power.

at the ground. Table 4 summarizes the different possibilities. In the two- and one-photon excitations, the modeless laser (type III) gives the best results because the laser transitions considered are strongly saturable. The saturation intensities involved are

$$3S_{1/2} \rightarrow 3P_{3/2}: I_{13}^{\mathrm{Sat}} = \frac{h\nu_{589}}{\sigma_{01}\tau_3} \approx 185\ \mathrm{W/m^2},$$

$$3P_{3/2} \rightarrow 4D_{5/2}: I_{36}^{\mathrm{Sat}} = \frac{h\nu_{569}}{\sigma_{02}\tau_{6,3}} \approx 475\ \mathrm{W/m^2},$$

$$3S_{1/2} \rightarrow 3P_{3/2}: I_{15}^{\mathrm{Sat}} = \frac{h\nu_{330}}{\sigma_0\tau_5} \approx 140\ \mathrm{W/m^2}.$$

For these three transitions, if the total laser power of, respectively, 15, 15, and 1 W excites only one velocity class, saturation parameters of, respectively, 190, 78, and 17 are obtained.

Table 4 shows the flux gain γ for different situations versus the normalized situation C_1 (two-photon excitation, two single-mode type I lasers of 2×15 W). A gain γ of 11 is obtained in the two-photon excitation with two modeless lasers of 2×15 W (see C_3 of Table 4). Likewise a notable result is that the same gain γ is obtained with only 1 W of a modeless laser at 330 nm in the one-photon excitation (see C_6). Figure 7 emphasizes this important result as a function of laser power. Consequently, the modeless lasers open a door of considerable interest to the use of 330 nm sodium excitation, which was rejected in Ref. 10 probably because of the strong saturation induced by a single-mode excitation (see C_4 of Table 4). Figure 6 displays the evolution of the photon flux at 330 nm Φ_{51}. A flux Φ_{51} of 4.2×10^4 photons/s/m^2 can be obtained in the two-photon excitation with two type III lasers of 2×15 W at 589 and 569 nm, and in the one-photon excitation with one type III laser of only 1 W at 330 nm (see C_3 and C_6 of Table 4). This flux is insufficient. But we can see in Fig. 6 that in the one-photon excitation, the average slope is $\eta_1=3\times10^4$ photons/s/m^2/W whereas in the two-photon excitation it is $\eta_2=1.3\times10^3$ photons/s/m^2/W, i.e., 20 times larger. This encouraging result shows that 10 W at 330 nm (one-photon excitation) is enough to produce a flux of 3×10^5 photons/s/m^2 whereas 400 W at 589 and 569 nm (two-photon excitation) produces only 1.8×10^5 photons/s/m^2 (see C_7 and C_8 of Table 4). The latter

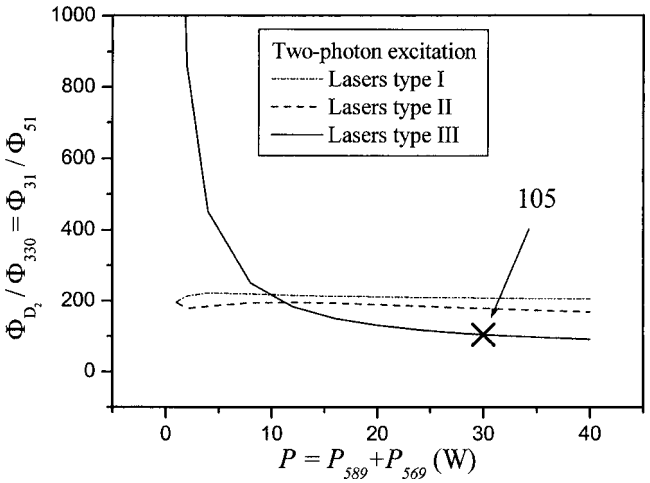

Fig. 8. Ratio between the returned flux at 589 and 330 nm as a function of total laser power in the two-photon excitation and for the three types of lasers: (i) type I, 1 MHz single-mode laser (dashed–dotted curve), (ii) type II, 1 MHz single-mode laser followed by a double phase modulation at 180 and 325 MHz (dashed curve), and (iii) type III, modeless laser (solid curve). The cross indicates that at 30 W total laser power (ELP-OA) the returned flux at 330 nm is at least 2 orders of magnitude smaller than at 589 nm.

laser power value cannot be attained at an astronomical site, whereas 10 W at 330 nm is much easier. Because the atmosphere's rate of change of refractive index with wavelength is strongest in the UV, the two-photon excitation as initially considered would require a very costly effort to reach the specification of Subsection 3.B. Fundamentally, the reason is that, in the two-photon excitation, the flux Φ_{51} at 330 nm is at least 2 orders of magnitude smaller than the flux Φ_{31} at 589 nm (D_2). Figure 8 displays the ratio $\Phi_{31}/\Phi_{51}(=\Phi_{D_2}/\Phi_{330})$ versus P for the two-photon excitation and for lasers types I, II, and III. For the value 30 W VIS in Fig. 6, which corresponds to the current ELP-OA program, using two modeless lasers of 2×20 W (2×15 W at the mesosphere), the theoretical fluxes Φ_{51} at 330 nm and ϕ_{31} at 589 nm are, respectively, and 4.4 $\times10^6$ photons/s/m^2. The flux ratio Φ_{D_2}/Φ_{330} of $\sim$105 is an intrinsic property of the sodium atom. This ratio Φ_{D_2}/Φ_{330} of $\sim$100 agrees very well with Ref. 29.

4. DISCUSSION

In the following, we consider the most favorable situation, corresponding to a type III laser with ELP-OA characteristics.

A. Two-Photon Excitation

The pulse delay and the power balance between the two lasers can be optimized. Figure 9 shows an optimum delay of 3.7 ns. A 10% gain is expected, but laser temporal jitter of a few nanoseconds implies gain losses of the same order of magnitude. Likewise, Fig. 10 shows an optimum gain of 10%, when the power is distributed in a ratio of 35% for the 589 nm laser and 65% for the 569 nm laser (case $P=30$ W). These gains are not sufficient to justify the extra development cost.

It was shown during the PASS-2 experiments that the radial superposition of the two laser beams was not better than 10%. This implies a flux decrease of 20%. Moreover, this superposition will be difficult to realize when the two lasers will have to follow the observation star. Indeed, we will have to consider the prism effect of the atmosphere that must be compensated in real time when the laser beam is launched in a direction away from the zenith. This is a major complication.

Without AO on the laser uplinks, the two laser spots at the mesosphere have a speckle structure when the beam size in the lower atmosphere is larger than r_0. The speckle structure, a function of wavelength, is different for each wavelength. As a result, the efficiency of the two-photon excitation could decrease.

As seen before, the two-photon excitation would need laser powers of hundreds of watts. Although the wavelength at 589 nm can be produced using solid-state lasers (frequency addition of two YAG[30] lasers or two fiber[31] lasers, Raman[32] laser, etc.), no solid-state lasers can gener-

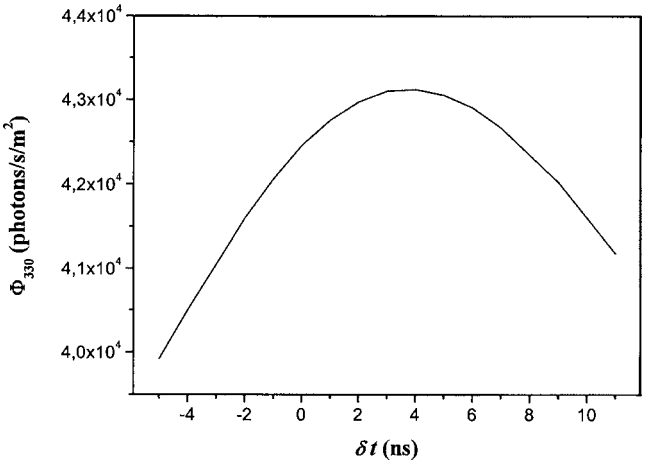

Fig. 9. Returned flux at 330 nm as a function of the delay between the 589 and 569 nm pulses in the two-photon excitation. A gain of 10% is expected for a 3.7 ns delay. Total laser power is 30 W.

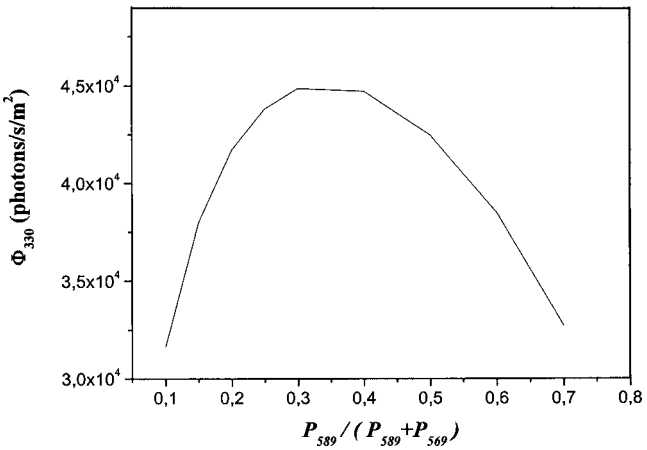

Fig. 10. Returned flux at 330 nm as a function of the ratio between 589 nm laser power and total laser power (589 and 569 nm) in the two-photon excitation. A gain of 10% is achieved when the power is distributed as a ratio of 35% at 589 nm and 65% at 569 nm. Total laser power is 30 W.

ate 569 nm. For now only dye lasers are available for these wavelengths with high power and high efficiency. Isotopic separation programs have demonstrated that it is possible to obtain 1000 W around 589 and 569 nm.[33] Moreover, around 100 W, the modeless laser starts again to raise the problem of saturation of sodium atom transitions.

Therefore, we see that in the two-photon excitation, there are several difficult technical limitations and there are few possibilities to significantly increase the flux of the chromatic components of the TTLGS. An incoherent excitation in the two-photon excitation with type III lasers allows a maximum population transfer of 7% for 2×15 W and 17% for 2×200 W in the $4D_{5/2}$ state. Only a coherent excitation with a theoretical transfer of population of 100% in the $4D_{5/2}$ state could allow a significant gain.[34] This solution is definitely difficult to implement on the sky and at an astronomical site because it requires ultrafast lasers, with energies per pulse of approximately a few microjoules per square centimeter, which implies, at the mesosphere, mean powers approaching 100 W with the required spot size and laser repetition rate. Many technical problems will probably result in a transfer significantly weaker than 100%.

B. One-Photon Excitation

The direct excitation of $4P_{3/2}$ at 330 nm is more promising for several reasons. First, this solution is fundamentally more efficient because only one 1 W laser of type III allows a transfer of 3% to the sodium state $4P_{3/2}$ and 20% for 10 W. It is well known that assuming a two-level absorption transition, the maximum population transfer can be 50% using simply incoherent excitation. Let us recall that a flux Φ_{51} of 3×10^5 photons/s/m^2 is achieved in the conditions defined in Subsection 3.B: 10 W laser of type III (in the mesosphere), $f_L=17$ kHz, $\Delta t=50$ ns, $w=0.4$ m, $\rho=4\times10^9$ atoms/cm^2. Many parameters can allow the optimization of the returned flux. For example, a 10 W quasi-cw laser at 330 nm would give a photon flux Φ_{51} of 4.5×10^5 photons/s/m^2 (see C_9 in Table 4). This value is 1 order of magnitude larger than the flux value Φ_{51} of 4.2×10^4 photons/s/m^2 obtained from two lasers of 2×15 W (in the mesosphere) of type III for the current ELP-OA project.

Despite the weaker atmospheric transmission at 330 nm on a good astronomical site (40%–50% instead of 80% at 589 nm), a 2–2.5 W modeless laser (at the ground) is enough to equal the current solution considered by ELP-OA and a modeless laser of 20–25 W would provide a flux ten times more intense. Contrary to the 589 and 569 nm case, for 330 nm there exists efficient solutions using solid-state lasers. A quasi-cw laser of 10 W at 355 nm with $M^2<1.2$ is already available commercially. There are solid-state systems such as Nd:YAG pumped by laser diodes and frequency tripling.[35] Nd-doped YAG or YLF matrix lasers have an intense laser line at 1321 nm. Nd:YLF has its maximum gain at 1321 nm. We can obtain the laser line at 330 nm (Ref. 36) in the previous case using frequency quadrupling. High-power optical fiber lasers at 1321 nm can be developed. We can also achieve frequency addition of frequency doubling of a 532 nm Nd:YAG with a 870 nm Sa:Ti laser or high-power laser diodes. UV laser diode progress is also promising. Laser diodes working directly at 375 nm are commercially available. Other solutions already exist. While waiting for solid-state sources to be developed, we can easily use a frequency-doubling high-yield DCM dye laser at 660 nm to obtain powers higher than 10 W at 330 nm.

Another important advantage is the simplification at an astronomical site. The solution that we propose does not modify the monochromatic LGS facilities already working on very large telescopes. For tip–tilt correction it is sufficient to replace the TTNGS by a TTLGS produced by an independent laser at 330 nm. The TTLGS can be positioned anywhere in the isoplanatic patch. It is not necessary to extract the superimposed component D_2 and at least two UV–VIS–IR components of the PLGS. This is a gain in simplicity and yield. For example, no grating is needed to extract the D_1 and the D_2 components, as in the case of PASS-1 and PASS-2. Furthermore, in the two-photon excitation, the D_2 line has two components: One comes from the one-photon excitation at 589 nm (LGS) and the other from the radiative cascade (TTLGS) (see Figs. 1 and 2). The latter would be useful to measure $\Delta\theta$. However, they cannot be separated. Thus, to measure $\Delta\theta$ in the one-photon excitation, the D_2 component can be used together with the D_1 component, which doubles the returned flux at 589 nm and eliminates the use of a grating.

The technical problems of spatial superimposing and time synchronization evoked above disappear because the two lasers that produce a TTLGS and LGS are independent. This means better reliability. Additional flexibility is provided by the choice of laser repetition rates. Indeed, the atmospheric coherence times of the wavefront and of the tip–tilt are

$$\tau_{0,\text{wavefront}} = r_0/\Delta v, \tag{15}$$

$$\tau_{0,\text{tilt}} = 12.33\left(\frac{D}{r_0}\right)^{1/6}\left(\frac{r_0}{v}\right), \tag{16}$$

where r_0 is the Fried parameter, D is the telescope diameter, and v is the wind velocity. In the VIS range (~0.5 μm) and for telescopes of 8–10 m range, $\tau_{0,\text{wavefront}}$ and $\tau_{0,\text{tilt}}$ are about 10 and 100 ms, respectively. As a result, the 330 nm laser that produces the TTLGS can have a repetition rate ten times lower than the one at 589 nm used for high-order correction. This possibility could be of interest. For example, to increase the returned flux, $4P_{3/2}$ direct excitation could also be produced by an ultrafast laser for 100% transfer of the ground-state population to the excited-state $4P_{3/2}$ using laser coherent transfer or chirped laser adiabatic transfer. The essential point for 100% transfer is the required energy per pulse that must be of the order of few microjoules per square centimeter. At a 17 kHz repetition rate this implies huge mean laser powers (850 W for a 1 m^2 spot, 5 μJ/cm^2 and a repetition rate of 17 kHz). Then we could think that the laser repetition rate can be decreased until it becomes inversely proportional to the tip–tilt coherence time, to reach the required energy per laser pulse for the same average power. However, in terms of photon flux per second, it is clear that to keep 100% of a population in the excited

state for each laser pulse during time dt at 1 kHz is equivalent to maintaining a 10% population during time dt at 10 kHz. The cost and technical difficulties determine the choice.

Another question is the angular extent of the laser beam versus wavelength. Atmospheric turbulence limits beam propagation. The Fried parameter r_0 varies with wavelength: $r_0 \propto \lambda^{6/5}$. An average value of the Fried parameter r_0 at a good astronomical site is $\sim$10 cm at 589 nm and 5 cm at 330 nm. If the laser beam size is close to or larger than r_0, angular spot size is limited by the seeing λ/r_0. The seeing varies slowly with λ as $\lambda^{-1/5}$. This means that a spot size at the mesosphere needs a projector of approximately the same diameter at 589–569 and 330 nm.

If the noise in measuring $\Delta\theta$ was dominated by Rayleigh residual scattering of atoms and molecules of the higher atmosphere observed in the telescope field of view, we could think that the solution presented in the one-photon excitation would be worse from this point of view. However, this is not the case. Indeed, Rayleigh scattering increases as $\eta_R = (P_{330}/P_{589})(\lambda_{589}/\lambda_{330})^4$. The one-photon excitation, involving a lower laser power, is in fact more convenient. For 1 W at 330 nm and 30 W at 589 and 569 nm, η_R is 0.3, and for 10 W at 330 nm and 400 W at 589 and 569 nm, η_R is 0.25. For an identical returned flux, Rayleigh scattering is thus three or four times weaker in the one-photon excitation. Moreover, we will demonstrate in a future paper[37] that, thanks to the modeless laser, Rayleigh scattering can be eliminated.

Finally one may expect that, on new generation telescopes, telescope vibration will be negligible and the optical axes will be stable. As a result, the UV beam could be projected into the mesosphere by the telescope itself. Thus, the measurement of $\Delta\theta$ will not require measurement of the centroid of the UV component of the TTLGS because, thanks to the light principle of reverse return light, the centroid of the UV component will not move. The measurement of only one VIS or IR chromatic component will thus be enough. This will represent a gain factor of 2 in calculation time and an additional simplification in the optical system of observation.

5. CONCLUSION

The calculations using the model presented in this paper are in good agreement with the experimental results on the sky at Keck, the LLNL, and Pierrelatte. Our model clearly shows that the new solution suggested (one-photon excitation), which consists in exciting sodium atoms with one 330 nm photon, needs only 1 W from a modeless laser to produce a returned flux of 4.2×10^4 photons/s/m^2 at 330 nm. This flux is equivalent to that obtained by an excitation with two photons using two modeless lasers operating at 589 and 569 nm of 15 W each (two-photon excitation). The flux that is required for the measurement of the differential tip–tilt $\Delta\theta$ is the main issue addressed in this paper. Taking the coherence time of the atmospheric tip–tilt into account, θ must be corrected at a frequency close to 100 Hz. Under these conditions only a measurement of the centroid of the chromatic components of a TTLGS will be possible at this speed. The two-photon excitation flux is then largely insufficient because one would have only a few hundred photons for the measurement of the centroid, which must be of extreme precision. We showed that a returned flux at 330 nm ranging between 2×10^5 photons/s/m^2 and 1.3×10^6 photons/s/m^2 is necessary. Our calculations clearly show that a modeless laser or quasi-continuous laser of 10 W operating at 330 nm makes it possible to meet the requirement, whereas one would need more than 2×200 W at 589 nm + 569 nm. To validate this proposal, experiments in the laboratory are in progress.

The solution suggested also has other advantages:

1. Two completely independent lasers at 330 and 589 nm provide a richer choice of technologies. All solid-state lasers are then possible. One of the major disadvantages of the two-photon excitation is the wavelength at 569 nm that does not have, to our knowledge, any solid-state laser solution. It thus imposes dye lasers for the two wavelengths because they must have rigorously identical characteristics.
2. The independence of the LGS and the TTLGS greatly simplifies the system and allows an upgrade without significant modification to the existing LGS. The problems of tip–tilt and higher-order corrections can then be optimized more easily and separately. To obtain a sufficient intensity at 330 nm, the two-photon excitation would require a power of more than 200 W for the 589 nm laser. But such a power is useless for the production of a LGS; 20 W is enough.
3. The 330 nm laser power to be implemented is relatively low and thus amenable to very compact solid-state systems that would be fixed directly on the telescope. It would not then be necessary to transport the beam over large distances.

ACKNOWLEDGMENTS

We thank Celine d'Orgeville and Francois Rigaut of Gemini and Marcos van Dam of Keck for helpful discussions. The authors also express thanks to Derick Salmon of the Canada–France–Hawaii Telescope for careful reading of the manuscript and helpful suggestions. This work was supported by the CNRS.

Corresponding author J.-P. Pique's e-mail address is pique@spectro.ujf.grenoble.fr; phone, 33-476-514-745.

REFERENCES

1. A. R. Contos, P. L. Wizinowich, S. K. Hartman, D. Le Mignant, C. R. Neyman, P. J. Stomski, and D. Summers, "Laser guide star adaptive optics at the Keck Observatory," in *Adaptive Optical System Technologies II*, P. L. Wizinowich and D. Bonaccini, eds., Proc. SPIE **4839**, 370–380 (2003).
2. D. Bonaccini, W. Hackenberg, M. Cullum, E. Brunetto, T. Ott, M. Quattri, E. Allaert, M. Dimmler, M. Tarenghi, A. Van Kersteren, C. Di Chirico, B. Buzzoni, P. Gray, R. Tamai, and M. Tapia, "ESO VLT laser guide star facility," in *Adaptive Optics Systems and Technology II*, R. K. Tyson, D. Bonaccini, and M. C. Roggemann, eds., Proc. SPIE **4494**, 276–289 (2002).
3. C. d'Orgeville, B. Bauman, J. Catone, B. Ellerbroek, D. Gavel, and R. Buchroeder, "Gemini north and south laser

guide star systems requirements and preliminary designs," in *Adaptive Optics Systems and Technology II*, R. K. Tyson, D. Bonaccini, and M. C. Roggemann, eds., Proc. SPIE **4494**, 302–316 (2002).
4. J. Drummond, J. Telle, C. Denman, P. Hilman, and A. Tuffli, "Photometry of a sodium laser guide star at Starfire Optical Range," Publ. Astron. Soc. Pac. **116**, 278–289 (2004).
5. S. S. Olivier, C. E. Max, H. W. Friedman, J. An, K. Avicola, B. V. Beeman, H. D. Bissinger, J. M. Brase, G. V. Erbert, D. T. Gavel, K. Kanz, B. Macintosh, K. P. Neeb, and K. E. Waltjen, "First significant image improvement from a sodium-layer laser guide star adaptive optics at Lick Observatory," in *Adaptive Optics and Applications*, R. K. Tyson and R. Q. Fugate, eds., Proc. SPIE **3126**, 240–248 (1997).
6. P. L. Wizinovich, D. Le Mignant, A. H. Bouchez, R. D. Campbell, J. C. Y. Chin, A. R. Contos, M. A. van Dam, S. K. Hartman, E. M. Johansson, R. E. Lafon, H. Lewis, P. J. Stomski, D. M. Summers, C. G. Brown, P. M. Danforth, C. E. Max, and D. Pennington, "The W. M. Keck Observatory laser guide star adaptive optics system: overview," Publ. Astron. Soc. Pac. **118**, 297–309 (2006).
7. I. S. McLean and S. Adkins, "Instrumentation at the Keck Observatory," in *Ground-based Instrumentation for Astronomy*, A. F. M. Moorwood, and M. Iye, eds., Proc. SPIE **5492**, 1–12 (2004).
8. R. Foy and J. P. Pique, "Lasers in astronomy," in *Handbook of Laser Technology and Applications*, C. E. Webb and J. D. C. Jones, eds. (Institute of Physics, 2004), Vol. 1, pp. 2581–2624.
9. R. Foy, CNRS (personal communication, 2005).
10. R. Foy, A. Migus, F. Biraben, G. Grynberg, P. R. McCullough, and M. Tallon, "The polychromatic artificial sodium star: a new concept for correcting the atmospheric tilt," Astron. Astrophys., Suppl. Ser. **111**, 569–578 (1995).
11. The term "modeless" was first introduced by P. Ewart in 1985 and then used by K. Bergmann in 1992 because the mode structure of the cavity is canceled (see Ref. 12).
12. J. P. Pique and S. Farinotti, "An efficient modeless laser for a mesospheric sodium laser guide star," J. Opt. Soc. Am. B **20**, 2093–2101 (2003).
13. M. Schöck, R. Foy, M. Tallon, L. Noethe, and J. P. Pique, "Performance analysis of polychromatic laser guide stars used for wave front tilt sensing," Mon. Not. R. Astron. Soc. **337**, 910–920 (2002).
14. C. d'Orgeville and F. Rigaut, Gemini (personal communication, 2005).
15. M. A. van Dam, A. H. Bouchez, D. Le Mignant, E. M. Johansson, P. L. Wizinowich, R. D. Campbell, J. C. Y. Chin, S. K. Hartman, R. E. Lafon, P. J. Stomski, Jr., and D. M. Summers, "The W. M. Keck Observatory laser guide star adaptive optics system: performance characterization," Publ. Astron. Soc. Pac. (to be published).
16. J. Vaillant, E. Thiebaut, and M. Tallon, "ELPOA: data processing of chromatic differences of the tilt measured with a polychromatic laser guide star," in *Adaptive Optical Systems Technology*, P. L. Wizinowich, ed., Proc. SPIE **4007**, 308–315 (2000).
17. G. Mégie, F. Bos, J. E. Blamont, and M. L. Chanin, "Simultaneous nighttime LIDAR measurements of atmospheric sodium and potassium," Planet. Space Sci. **26**, 27–35 (1978).
18. K. H. Kwon, D. C. Senft, and C. S. Gardner, "Lidar observations of sporadic sodium layers at Mauna Kea Observatory, Hawaii," J. Geophys. Res. **93**, 14199–14208 (1988).
19. L. Michaille, J. B. Clifford, J. C. Dainty, T. Gregory, J. C. Quartel, F. C. Reavell, R. W. Wilson, and N. J. Wooder, "Characterization of the mesospheric sodium layer at La Palma," Mon. Not. R. Astron. Soc. **328**, 993–1000 (2001).
20. C. S. Gardner and J. D. Shelton, "Density response of neutral atmospheric layer to gravity wave perturbations," J. Geophys. Res. **90**, 1745–1754 (1985).
21. C. W. Allen, *Astrophysical Quantities* (Athlone, 1973), pp. 25–26.
22. J. Drummond, J. Telle, C. Denman, P. Hillman, J. Spinhirne, and J. Christou, "Photometry of a sodium laser guide star from the Starfire Optical Range. II. Compensating the pump beam," Publ. Astron. Soc. Pac. **116**, 952–964 (2004).
23. M. Schöck, J. P. Pique, A. Petit, P. Chevrou, V. Michau, G. Grynberg, A. Migus, N. Ageorges, V. Bellanger, F. Biraben, R. Deron, H. Fews, R. Foy, C. Högemann, M. Laubscher, D. Müller, C. d'Orgeville, O. Peillet, M. Redfern, F. Foy, P. Segonds, R. Soden, M. Tallon, E. Thiebaut, A. Tokovinin, J. Vaillant, and J. M. Weulersse, "ELP-OA: measuring the wavefront tilt without a natural guide star," in *Propagation and Imaging through the Atmosphere IV*, M. C. Roggemann, ed., Proc. SPIE **4125**, 41–52 (2000).
24. R. Foy, J. P. Pique, A. Petit, P. Chevrou, V. Michau, V. Prigent, G. Grynberg, A. Migus, N. Ageorges, V. Bellanger, F. Biraben, R. Deron, H. Fews, F. Foy, C. Högemann, P. Jajourel, M. Laubscher, D. Müller, C. d'Orgeville, O. Peillet, M. Redfern, M. Schöck, P. Segonds, R. Soden, M. Tallon, I. Tallon-Bosc, E. Thiebaut, A. Tokovinin, J. Vaillant, and J. M. Weulersse, "ELP-OA: toward the tilt measurement from a polychromatique laser guide star," in *Adaptive Optical Systems Technology*, P. L. Wizinowich, ed., Proc. SPIE **4007**, 287–299 (2000).
25. R. Foy, J. P. Pique, A. Petit, P. Chevrou, V. Michau, V. Prigent, G. Grynberg, A. Migus, N. Ageorges, V. Bellanger, F. Biraben, R. Deron, H. Fews, F. Foy, C. Högemann, P. Jajourel, M. Laubscher, D. Müller, C. d'Orgeville, O. Peillet, M. Redfern, M. Schöck, P. Segonds, R. Soden, M. Tallon, I. Tallon-Bosc, E. Thiebaut, A. Tokovinin, J. Vaillant, and J. M. Weulersse, "Polychromatic guide star: feasibility study," in *High Power Laser Ablation III*, C. R. Phipps, ed., Proc. SPIE **4065**, 312–324 (2002).
26. R. Foy, M. Tallon, I. Tallon-Bosc, E. Thiébaut, J. Vaillant, F. C. Foy, D. Robert, H. Friedman, F. Biraben, G. Grynberg, J. P. Gex, A. Mens, A. Migus, J. M. Weulerse, and D. J. Butler, "Photometric observations of a polychromatic laser guide star," J. Opt. Soc. Am. A **17**, 2236–2242 (2000).
27. C. E. Max, K. Avicola, J. M. Brase, H. W. Friedman, H. D. Bissinger, J. Duff, D. T. Gavel, J. A. Horton, R. Kiefer, J. R. Morris, S. S. Olivier, R. W. Presta, D. A. Rapp, J. T. Salmon, and K. E. Waltjen, "Design, layout, and early results of a feasibility experiment for sodium-layer laser-guide-star adaptive optics," J. Opt. Soc. Am. A **11**, 813–824 (1994).
28. G. Froc, E. Rosencher, B. Attal-Trétout, and V. Michau, "Photon return analysis of a polychromatic laser guide star," Opt. Commun. **178**, 405–409 (2000).
29. V. Bellanger, A. Courcelle, and A. Petit, "A program to compute the two-step excitation of mesospheric sodium atoms for the Polychromatic Laser Guide Star Project," Comput. Phys. Commun. **162**, 143–150 (2004).
30. C. A. Denman, P. D. Hillman, G. T. Moore, J. M. Telle, J. D. Drummond, and A. L. Tuffli, "20W, CW 589 nm sodium beacon excitation source for adaptive optical telescope application," Opt. Mater. **26**, 507–513 (2004).
31. D. M. Pennington, J. W. Dawson, A. Drobshoff, Z. Liao, S. Payne, D. Bonaccini, W. Hackenberg, and L. Taylor, "Compact fiber laser approach to 589 nm laser guide stars," in *Conference on Lasers and Electro-Optics*, Vol. 2 of 2004 OSA Technical Digest Series (Optical Society of America, 2004), p. 1.
32. W. Hackenberg and D. Bonaccini, "Fiber Raman laser development for multiconjugate adaptive optics with sodium laser guide stars," in *Adaptive Optics System and Technology II*, R. K. Tyson, D. Bonaccini, and M. C. Roggermann, eds., Proc. SPIE **4494**, 271–275 (2002).
33. K. Avicola, J. M. Brase, J. R. Morris, H. D. Bissinger, J. M. Duff, H. W. Friedman, D. T. Gavel, C. E. Max, S. S. Olivier, R. W. Presta, D. A. Rapp, J. T. Salmon, and K. Valtjen, "Sodium-layer laser-guide-star experimental results," J. Opt. Soc. Am. A **11**, 825–831 (1994).

34. J. Biegert and J. C. Diels, "Feasibility study to ceate a polychromatic guidestar in atomic sodium," Phys. Rev. A **67**, 043403/1-11 (2003).
35. S. Fournier, "Quelques technologies laser récentes et leurs applications," Photoniques **18**, 25–27 (2005).
36. Y. Louyer, F. Balembois, M. D. Plimmer, T. Badr, P. Georges, P. Juncar, and M. E. Himbert, "Efficient cw operation of diode-pumped Nd:YLF lasers at 1312.0 and 1322.6 nm for a silver atom optical clock," Opt. Commun. **217**, 357–362 (2003).
37. H. Guillet de Chatellus, I. C. Moldovan, V. Fesquet, and J. P. Pique, "Suppression of the Rayleigh scattering noise in sodium laser guide stars by hyperfine depolarization of the fluorescence,"Opt. Express (to be published).